CHANNEL MODEL OF A STRONG-CURRENT DISCHARGE IN A RAILGUN

S. V. Kukhtetskii

UDC 533.9

The "plasma piston" model [1, 2] is often employed in the theoretical analysis of the operation of some MHD devices with a localized discharge. However, experiments performed on a railgun with an external magnetic field showed that at high pressures ($p_\infty < 25$ kPa) the measured value of the discharge velocity is significantly higher than the value calculated based on the piston model [3]. In later experiments on the same setup and on a longer channel it was found that there exist two stages of the motion of the discharge already after the discharge current becomes stationary. At first it fills the entire transverse section of the channel, and the elevated velocity can be explained by the partial leakage of the gas swept up into the current-carrying region [4]. Then, after 20-25 cm, the discharge is compressed in the transverse direction and then moves so as to fill not more than 50-60% of the channel cross section [5]. At the same time the flow of part of the pushed gas around the current region becomes significant.

Detailed analysis of the structure of the flow, which is a difficult problem even for flow around a solid nondeformable body, becomes even more complicated in this case because the shape of the discharge in the flow, being very irregular, in its turn depends on the parameters of the flow. In this connection, in this work an attempt is made to take into account the flow around the discharge in the simplest quasi-one-dimensional stationary formulation under the following assumptions.

1. The entire region behind the shock wave (Fig. 1) can be divided into three quasi-one-dimensional zones: the zone of isentropic flow 1 exterior relative to the discharge, the thin thermal layer 2 at the discharge-gas boundary (transforming into the thermal wake behind the discharge), and the current region itself 3.†

2. The thermal layer consists of a dissociated and discharge-heated gas whose degree of ionization is much lower than in the current-carrying region, while the velocity of the gas in it equals the velocity of the external isentropic flow. Unlike the region 1, however, the velocity in the wake is subsonic, as a result of which the back end wall of the accelerator 4 has a significant effect on the parameters of the entire flow. The thermal layers are assumed to be thin, so that other effects associated with the presence of these layers, such as expulsion, etc., are ignored.

3. Convective processes in the discharge 3 are ignored, and the energy balance is calculated in two limiting cases: optically thin plasma, when all of the Joule heat liberated in the discharge is carried away by the volume radiation, and optically dense plasma, when the discharge emits from the surface as an absolutely black body. The energy of the radiation is absorbed in the thermal layer and is carried away downstream.

4. The possible detachment of the flow and a vortex in the tail part of the discharge have no effect on the integral characteristics of the process, since, as will be shown below, the main pressure drop (and, therefore, the contribution to the resistance force) occurs in the region where the curvature of the side edge of the discharge is small.

Thus the scheme of the flow is as follows (see Fig. 1). The supersonic flow with the velocity u_∞, known pressure p_∞ and density ρ_∞ is decelerated at the front of the shock wave 5, moving away from the discharge with a velocity D, where a_0 is the half-width of the channel, $a(x)$ is the half-width of the current-carrying region in the flow, and $0 \le x \le l$. All sections are taken per unit height of the channel h. After the shock wave the flow in the region 1 is analogous to the flow in a Laval nozzle with the critical section $a_0 - a*$ and equal inlet and outlet sections a_0. The parameters of the gas at the inlet to the nozzle are u_0, p_0, and ρ_0, while the parameters at the outlet are u_1, p_1, and ρ_1. In the region $0 \le x \le l$, the velocity of the gas, the pressure, and

†In Fig. 1 and below the reference system is tied to the discharge.

Krasnoyarsk. Translated from Zhurnal Prikladnoi Mekhaniki i Tekhnicheskoi Fiziki, No. 3, pp. 30-36, May-June, 1987. Original article submitted March 14, 1986.

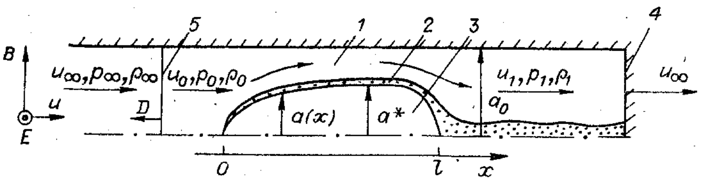

Fig. 1

the density equal u(x), p(x), and ρ(x). Using the well-known formulas [6] for isentropic flow in a channel with a variable cross section

$$\left(1-\frac{a}{a_0}\right)^2=\frac{M_0^2}{M^2}\left(\frac{1+\frac{\gamma-1}{2}M^2}{1+\frac{\gamma-1}{2}M_0^2}\right)^{\frac{\gamma+1}{\gamma-1}} \text{ and } \frac{p}{p_0}=\left(\frac{1+\frac{\gamma-1}{2}M_0^2}{1+\frac{\gamma-1}{2}M^2}\right)^{\frac{\gamma}{\gamma-1}}, \tag{1}$$

the condition M = 1 for $a = a^*$ and equal inlet and outlet sections, we have

$$\left(1-\frac{a^*}{a_0}\right)^2=\frac{\left(\frac{\gamma+1}{\gamma-1}\right)^{\frac{\gamma+1}{\gamma-1}}M_0^2}{\left(\frac{2}{\gamma-1}+M_0^2\right)^{\frac{\gamma+1}{\gamma-1}}}=\frac{\left(\frac{1}{M_1^2}\right)^{\frac{2}{\gamma-1}}\left(\frac{\gamma+1}{\gamma-1}\right)^{\frac{\gamma+1}{\gamma-1}}}{\left(1+\frac{2}{\gamma-1}\frac{1}{M_1^2}\right)^{\frac{\gamma+1}{\gamma-1}}}; \tag{2}$$

$$\frac{p_1}{p_0}=\left(\frac{M_0^2}{M_1^2}\right)^{\frac{\gamma}{\gamma+1}} \tag{3}$$

Here M = u/c is Mach's number and γ is the adiabatic index. From (1), eliminating M and using (2) and (3), the form of the discharge a(x) can be related with the pressure p(x):

$$\frac{a}{a_0}=1-\frac{\left(\frac{p_1}{p_0}\right)^{\frac{1}{\gamma}}\left(1-\left(\frac{p_1}{p_0}\right)^{\frac{\gamma-1}{\gamma}}\right)^{1/2}}{\left\{\left[1-\left(\frac{p_1}{p_0}\right)^{\frac{\gamma+1}{\gamma}}\right]\left(\frac{p}{p_0}\right)^{\frac{2}{\gamma}}-\left[1-\left(\frac{p_1}{p_0}\right)^{\frac{2}{\gamma}}\right]\left(\frac{p}{p_0}\right)^{\frac{\gamma+1}{\gamma}}\right\}^{1/2}}. \tag{4}$$

In the stationary case the pressure distribution in the region 1 must be identical to that in the discharge, and the pressure gradient in the discharge is balanced by the force jB (j is the current density and B is the magnetic induction). Thus

$$\partial p/\partial x=-jB,\ 0\leqslant x\leqslant l. \tag{5}$$

Multiplying both sides of (5) by a(x) and integrating over x we find

$$\int_0^l a\frac{\partial p}{\partial x}dx=-a_0p_0\int_{p_1/p_0}^1\frac{a}{a_0}d\left(\frac{p}{p_0}\right)=-B\int_0^l jadx=-\frac{1}{2}IB$$

(I is the total discharge current) or in dimensionless form

$$\frac{IB}{2a_0p_\infty}\frac{p_\infty}{p_0}=\int_{p_1/p_0}^1\frac{a}{a_0}d\left(\frac{p}{p_0}\right). \tag{6}$$

Substituting into (6) the expression (4) and carrying out the integration we obtain

$$\frac{p_0}{p_\infty}=\frac{\frac{IB}{2a_0p_\infty}}{1-\frac{p_1}{p_0}-\frac{2\gamma}{\gamma-1}\frac{\left(\frac{p_1}{p_0}\right)^{1/\gamma}-\frac{p_1}{p_0}}{1+\left(\frac{p_1}{p_0}\right)^{1/\gamma}}}. \tag{7}$$

Using the Hugoniot relation at the shock-wave front it is easy to relate the velocity of the incident flow $M_\infty = u_\infty/c_\infty$ with p_0/p_∞:

$$M_\infty = \frac{c_0}{c_\infty} M_0 + \frac{\frac{p_0}{p_\infty} - 1}{\left[\frac{\gamma(\gamma-1)}{2}\left(\frac{\gamma+1}{\gamma-1}\frac{p_0}{p_\infty} + 1\right)\right]^{1/2}}, \tag{8}$$

where c_0/c_∞ is the ratio of the velocity of sound behind the shock wave front to the velocity of sound in the incident flow, expressed in terms of p_0/p_∞. Based on the foregoing remark about the thermal wake it can be assumed that in the stationary case the velocity of the gas u_1 will equal the velocity of the back end wall of the accelerator, i.e., $u_1 = u_\infty$, in spite of the fact that $M_1 = u_1/c_1 > 1$. In dimensionless form

$$M_1 \frac{c_1}{c_0} \frac{c_0}{c_\infty} = M_\infty. \tag{9}$$

From the condition that the flow in region 1 should be isentropic we have

$$\frac{c_1}{c_0} = \left(\frac{p_1}{p_0}\right)^{\frac{\gamma-1}{2\gamma}}. \tag{10}$$

Eliminating M_1, M_0, and M_∞ from (2), (3), (8), (9), and (10) we obtain

$$\frac{\left[1 - \left(\frac{p_1}{p_0}\right)^{\frac{\gamma-1}{\gamma}}\right]\left[1 - \left(\frac{p_1}{p_0}\right)^{\frac{1}{\gamma}}\right]}{1 + \left(\frac{p_1}{p_0}\right)^{\frac{1}{\gamma}}} = \frac{\left(\frac{p_0}{p_\infty} - 1\right)^2}{\gamma \frac{p_0}{p_\infty}\left(\frac{\gamma+1}{\gamma-1} + \frac{p_0}{p_\infty}\right)}. \tag{11}$$

The solution of this equation together with (7) gives the dependence of p_1/p_0 on the parameter $IB/2a_0p_\infty$, and knowing p_1/p_0 it is easy to calculate based on the formulas presented above all parameters of the flow outside the discharge in the region $x \le 0$ and $x \ge l$. Figure 2 shows the dependence of M_∞ (in the laboratory coordinate system M_∞ is the dimensionless velocity of the discharge) and p_1/p_0 on $IB/2a_0p_\infty$ for $\gamma = 1.667$, 1.4, 1.333, and 1.2 (lines 1-4).

The values of p_1/p_0 give the necessary boundary conditions for solving Eq. (5). For accelerators of dense gases with external magnetic fields $B \sim 1$-2 T and discharge currents $I \sim 10$-40 kA the induced electric field uB is several times weaker than the external field E and can be neglected. Thus $j = \sigma E$ (σ is the conductivity of the plasma). Assuming that the plasma is uniform along the current (along the z axis) and taking into account the fact that the conductivity of the electrodes is much higher than the conductivity of the plasma, we find that E is independent of x. Therefore to solve (5) it is necessary to specify only the dependence of σ on p. For this, we shall examine the energy balance in the current-carrying region.

1. Optically Thin Plasma. The characteristic time of the process in the accelerator $\sim 10^{-4}$-10^{-3} sec, so that on spatial scales $\gtrsim 1$-10 cm the effect of heat conduction can be neglected. Since convective processes in the current-carrying region are neglected, in the stationary case

$$\sigma E^2 = Q_R \text{ for } 0 \leqslant x \leqslant l, \ |y| \leqslant a(x). \tag{12}$$

In the general case the conductivity σ and the magnitude of the volume radiant losses Q_R are functions of the pressure p and temperature T. Since, however, the analysis carried out here is only of a qualitative character, we shall take into account the fact that σ depends weakly on p, and Q_R up to a factor of order unity can be represented in the form $Q_R(p, T) = pq_R(T)$, where q_R depends only on the temperature. We have

$$\sigma(T)E^2 = pq_R(T) \tag{13}$$

[$\sigma(T)$ and $q_R(T)$ are known functions]. Solving this equation for T and substituting into $\sigma(T)$ we find

$$\sigma = \sigma(p/E^2). \tag{14}$$

For pure air the dependence of σ on p/E^2 can be approximated well by the expression

$$\sigma = \alpha\left(\frac{p}{E^2}\right)^{-\beta}, \tag{15}$$

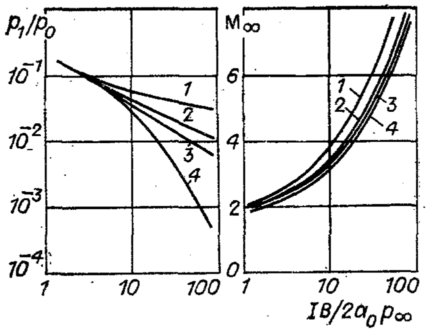

Fig. 2

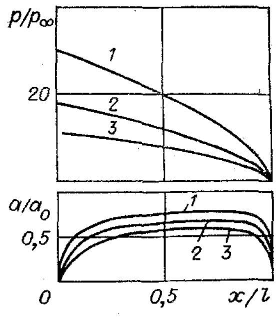

Fig. 3

where $\alpha = 0.27$ and $\beta = 0.71$, if σ is given in $\Omega \cdot$ cm, E in V/cm, and p in 10^5 Pa. Using (15) we obtain from (5)

$$\frac{\partial p}{\partial x} = -\sigma\left(\frac{p}{E^2}\right)EB = -\alpha\left(\frac{p}{E^2}\right)^{-\beta}EB. \tag{16}$$

Integrating (1) taking into account the fact that $p = p_0$ at $x = 0$ we have

$$\frac{1}{\beta+1}\left[1-\left(\frac{p}{p_0}\right)^{\beta+1}\right] = \frac{\alpha B E^{2\beta+1}}{p_0^{\beta+1}}x.$$

Since $p = p_1$ at $x = l$, we obtain finally

$$\frac{p}{p_0} = \left\{1-\left[1-\left(\frac{p_1}{p_0}\right)^{\beta+1}\right]\frac{x}{l}\right\}^{\frac{1}{\beta+1}}. \tag{17}$$

This expression permits finding the dependence of all remaining parameters of the flow on x/l in the region $0 \le x \le l$, as well as the form of the discharge a/a_0 from (4).

Figure 3 shows p/p_∞ and a/a_0 versus x/l for $\gamma = 1.4$ and $p_M = IB/2a_0p_\infty = 20$; 10; 5 (lines 1-3). We note that the curvature of the wide edge of the discharge is very small in the interval $0.1 \le x/l \le 0.95$. For large values of p_M the cross section of the discharge in the (x, y) plane is virtually rectangular. This can substantially simplify the analysis of processes occurring at the periphery of the discharge (the thermal layer 2, see Fig. 1), where the role of heat conduction will no longer be small. It is well known [7] that the resistance force of a body in a free flow at large Reynolds numbers is determined largely by the sharp drop in the pressure in the tail part of the body, caused by the detachment of the boundary layer and formation of eddy flow in the stagnation zone. In this case, for flow around a body in a channel, the pressure gradient along the flow is negative, so that detachment, in all probability, can occur only directly near the tail part, i.e., for $x/l \gtrsim 0.95$. As one can see from Fig. 3 only 10-15% of the total pressure drop in the flow occurs in the section $0.95 \le x/l \le 1$, so that taking detachment into account does not make a large contribution to the resistance force of the discharge.

The channel model of the discharge studied above in the approximation of an optically thin plasma contains one undetermined parameter – the length of the discharge l (or, which is equivalent, the electric field strength E), which must be obtained from experiment, or it is necessary to introduce the so-called ionization temperature [8], whose value in general is quite arbitrary. The choice of the local model of heat balance (12) and the neglecting of processes in the thermal boundary layer preclude the use of variational principles.

2. Optically Dense Plasma. Joule heat is carried out from the core of the discharge to the periphery by radiant heat conduction, is absorbed in the thermal layer, and carried away downstream. This is essentially the limiting case of convective heat exchange between the discharge and the gas flowing around it and can be regarded only as the upper limit of the energy losses in a railgun. As done previously, the thermal layer is assumed to be thin. In the case of an optically dense plasma the stationary temperature in the discharge T_d is identical in the entire region $0 \le x \le l$, $|y| \le a(x)$ and equals the temperature of the surface of the discharge. We have the following equation of force balance

$$\partial p/\partial x = -\sigma EB \approx \text{const} \tag{18}$$

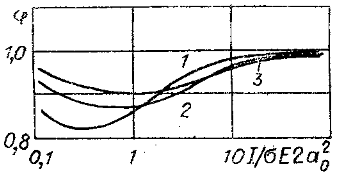

Fig. 4

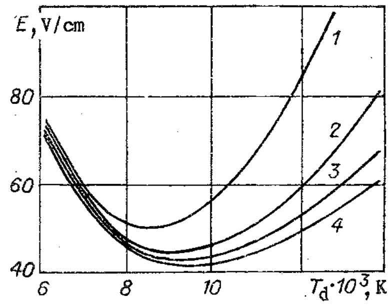

Fig. 5

and energy balance

$$hIE = \varepsilon\sigma_S T_d^4\left[2h\int_0^l \sqrt{1+\left(\frac{da}{dx}\right)^2}\,dx + 2\int_0^l a\,dx\right], \tag{19}$$

where σ_S is the Stefan–Boltzmann constant, h is the height of the discharge, and ε is the effective emissivity. The first term on the right side of (19) is the area of the lateral (in the flow) surface of the discharge, while the second term is the area of the regions near the electrodes. For simplicity we neglect other losses in the electrode. Making the substitution of variables $x \to p$ with the help of (18), we obtain in a dimensionless form

$$\frac{IE}{\varepsilon\sigma_S T_d^4 2a_0} = \int_{p_1/p_0}^{1}\left\{\left(\frac{2a_0p_0}{IB}\frac{I}{\sigma E2a_0^2}\right)^2 + \left(\frac{da/a_0}{dp/p_0}\right)^2\right\}^{1/2} d\left(\frac{p}{p_0}\right) +$$
$$+\frac{2a_0}{h}\frac{2a_0p_0}{IB}\frac{I}{\sigma E2a_0^2}\int_{p_1/p_0}^{1}\frac{a}{a_0}\,d\left(\frac{p}{p_0}\right)$$

or, using (6), we find

$$\frac{IE}{\varepsilon\sigma_S T_d^4 2a_0} = \int_{p_1/p_0}^{1}\left\{\left(\frac{2a_0p_0}{IB}\frac{I}{\sigma E2a_0^2}\right)^2 + \left(\frac{da/a_0}{dp/p_0}\right)^2\right\}^{1/2} d\,\frac{p}{p_0} + \frac{2a_0}{h}\frac{I}{\sigma E2a_0^2}. \tag{19'}$$

Here a/a_0 is expressed in terms of p/p_0 and p_1/p_0 from (4), $2a_0p_0/IB$ from (7), and p_1/p_0 from the solution of the exterior problem for fixed γ and $IB/2a_0p_\infty$. Thus, Eq. (19') gives a relationship between five dimensionless parameters of the form

$$\frac{IE}{\varepsilon\sigma_S T_d^4 2a_0} = \Phi\left(\frac{I}{\sigma E2a_0^2}, \frac{IB}{2a_0p_\infty}, \frac{2a_0}{h}, \gamma\right). \tag{20}$$

An analytic expression for Φ could not be derived, but this function is approximated well by a linear function of $I/\sigma E2a_0^2$:

$$\frac{IE}{\varepsilon\sigma_S T_d^4 2a_0} = \alpha\frac{I}{\sigma E2a_0^2} + \beta, \tag{21}$$

where

$$\alpha = \alpha\left(\frac{IB}{2a_0p_\infty}, \frac{2a_0}{h}, \gamma\right) = \frac{2a_0p_0}{IB}\left(1-\frac{p_1}{p_0}\right) + \frac{2a_0}{h};\quad \beta = 2\frac{a^*}{a_0},$$

a^* is the critical section of the discharge [see Fig. 1 and (2)]. Indeed, Fig. 4 shows the dependence of the ratio φ of the right sides of Eqs. (20) and (21) on $I/\sigma E2a_0^2$ for $\gamma = 1.4$ and $2a_0/h = 1$ ($p_M = IB/2a_0p_\infty$ = 2.5; 10; 40 – curves 1-3). One can see that the linear dependence differs by not more than 20% from the exact dependence. Using (21)

$$E=\frac{\varepsilon\sigma_S T_d^4 2a_0}{I}\left\{\frac{a^*}{a_0}+\left[\left(\frac{a^*}{a_0}\right)^2+\frac{\left(\frac{2a_0p_0}{IB}\left(1-\frac{p_1}{p_0}\right)+\frac{2a_0}{h}\right)I^2}{\sigma 2a_0^2\varepsilon\sigma_S T_d^4 2a_0}\right]^{1/2}\right\}. \quad (22)$$

Figure 5 shows this dependence for air for $\gamma = 1.4$, $2a_0 = 4$ cm, $2a_0/h = 1$, $\varepsilon = 1$, $IB/2a_0 p_\infty = 10$. At the same time $p_0/p_\infty = 17.94$, $p_1/p_0 = 0.0436$, and $a^*/a_0 = 0.687$. The curves 1-4 correspond to I = 10, 20, 30, and 40 kA. Since the radiant heat conduction is of a diffusive character and it is assumed that there are no convective flows in the current-carrying region, the discharge forms a dissipative system, for which the principle of minimum entropy production holds. In application to an electric arc it is known as Steenbeck's principle [9]. As one can see from Fig. 5, the curves $E = E(T_d)$ have distinct minima, which makes it possible, by using Steenbeck's principle, to determine T_d and E, thereby solving the problem completely. As one can see, the value of E varies in the range 40-50 V/cm, while T_d varies in the range 8500-9500 K. The power liberated in this case in a discharge of height h = 4 cm equals IEh and varies in the range 2-6.5 MW. The experimentally measured quantity IU ≈ IEh, neglecting the voltage drop at the electrodes, is of the same order of magnitude (~5 MW). It is difficult to make a detailed comparison with experiment, since for molecular gases the voltage on the electrodes undergoes strong pulsations, probably caused by the motion of the sections near the electrodes. The value of E in the discharge column was not measured directly.

The form of the discharge of an optically dense plasma is virtually identical to the case of a transparent plasma (see Fig. 3). The tail part is sharper, which is attributable to the linear dependence of p on x, and the flat profile for $0.1 \le x/l \le 0.9$ is just as distinct.

LITERATURE CITED

1. V. A. Derevyanko, V. S. Slavin, and V. S. Sokolov, "MHD generator based on the products of gasification of lignite," Zh. Prikl. Mekh. Tekh. Fiz., No. 5 (1980).
2. B. W. Boreham, "Study of travelling conduction wave accelerator," AIAA J., 14, No. 1 (1976).
3. S. V. Kukhtetskii, A. D. Lebedev, and V. A. Lyubochko, "Some characteristics of the motion of strong-current quasistationary discharge in a magnetic field," Abstracts of Reports at the 9th All-Union Conference on Low-Temperature-Plasma Generators, Ilim, Frunze (1983).
4. S. V. Kukhtetskii, A. D. Lebedev, and V. A. Lyubochko, "Motion of a strong-current discharge in a dense gas," Teplofiz. Vys. Temp., No. 3 (1985).
5. S. V. Kukhtetskii, V. A. Lyubochko, et al., "Integral model of a discharge in a railgun taking into account flow around the discharge," Zh. Prikl. Mekh. Tekh. Fiz., No. 1 (1986).
6. L. G. Loitsyanskii, Mechanics of Liquids and Gases [in Russian], Nauka, Moscow (1970).
7. G. Shlikhting, Boundary-Layer Theory [in Russian], Nauka, Moscow (1974).
8. Yu. P. Raizer, Foundations of the Modern Physics of Gas-Dynamic Processes [in Russian], Nauka, Moscow (1980).
9. V. Finkel'nburg and G. Mekker, Electric Arcs and Thermal Plasmas [Russian translation], IL, Moscow (1961).